

1 Drug resistance prediction for *Mycobacterium* 2 *tuberculosis* with reference graphs

3 1.1 Author names

4 Michael B. Hall^{1,2,*} (ORCID: [0000-0003-3683-6208](https://orcid.org/0000-0003-3683-6208)), Leandro Lima¹ (ORCID: [0000-0001-8976-2762](https://orcid.org/0000-0001-8976-2762)), Lachlan J. M. Coin² (ORCID: [0000-0002-4300-455X](https://orcid.org/0000-0002-4300-455X)), Zamin Iqbal^{1,*} (ORCID: [0000-0001-8466-7547](https://orcid.org/0000-0001-8466-7547))

7 1.2 Affiliation(s)

8 ¹European Molecular Biology Laboratory, European Bioinformatics Institute, Hinxton,
9 Cambridgeshire, United Kingdom

10 ²Department of Microbiology and Immunology, Peter Doherty Institute for Infection and
11 Immunity, The University of Melbourne, Melbourne, Australia

12 *Corresponding authors

13 1.3 Corresponding author and email address

14 Michael B. Hall: michael.hall2 [at] unimelb.edu.au

15 Zamin Iqbal: zi [at] ebi.ac.uk

16 1.4 Keywords

17 genome graphs, reference graphs, drug resistance prediction, *Mycobacterium tuberculosis*,
18 benchmark, software

19 2. Abstract

20 The dominant paradigm for analysing genetic variation relies on a central idea: all genomes
21 in a species can be described as minor differences from a single reference genome. However,
22 this approach can be problematic or inadequate for bacteria, where there can be significant
23 sequence divergence within a species.

24 Reference graphs are an emerging solution to the reference bias issues implicit in the “single-
25 reference” model. Such a graph represents variation at multiple scales within a population –
26 e.g., nucleotide- and locus-level.

27 The genetic causes of drug resistance in bacteria have proven comparatively easy to decode
28 compared with studies of human diseases. For example, it is possible to predict resistance to
29 numerous anti-tuberculosis drugs by simply testing for the presence of a list of single
30 nucleotide polymorphisms and insertion/deletions, commonly referred to as a catalogue.

31 We developed DrPRG (Drug resistance Prediction with Reference Graphs) using the bacterial
32 reference graph method Pandora. First, we outline the construction of a *Mycobacterium*
33 *tuberculosis* drug resistance reference graph, a process that can be replicated for other
34 species. The graph is built from a global dataset of isolates with varying drug susceptibility
35 profiles, thus capturing common and rare resistance- and susceptible-associated haplotypes.
36 We benchmark DrPRG against the existing graph-based tool Mykrobe and the haplotype-
37 based approach of TBProfiler using 44,709 and 138 publicly available Illumina and
38 Nanopore samples with associated phenotypes. We find DrPRG has significantly improved
39 sensitivity and specificity for some drugs compared to these tools, with no significant
40 decreases. It uses significantly less computational memory than both tools, and provides
41 significantly faster runtimes, except when runtime is compared to Mykrobe on Nanopore
42 data.

43 We discover and discuss novel insights into resistance-conferring variation for *M.*
44 *tuberculosis* - including deletion of genes *katG* and *pncA* – and suggest mutations that may
45 warrant reclassification as associated with resistance.
46

47 3. Impact statement

48 *Mycobacterium tuberculosis* is the bacterium responsible for tuberculosis (TB). TB is one of
49 the leading causes of death worldwide; before the coronavirus pandemic it was the leading
50 cause of death from a single pathogen. Drug-resistant TB incidence has recently increased,
51 making the detection of resistance even more vital. In this study, we develop a new software
52 tool to predict drug resistance from whole-genome sequence data of the pathogen using new
53 reference graph models to represent a reference genome. We evaluate it on *M. tuberculosis*
54 against existing tools for resistance prediction and show improved performance. Using our
55 method, we discover new resistance-associated variations and discuss reclassification of a
56 selection of existing mutations. As such, this work contributes to TB drug resistance
57 diagnostic efforts. In addition, the method could be applied to any bacterial species, so is of
58 interest to anyone working on antimicrobial resistance.

59 4. Data summary

60 **The authors confirm all supporting data, code and protocols have been provided within
61 the article or through supplementary data files.**

62 The software method presented in this work, DrPRG, is freely available from GitHub under
63 an MIT license at <https://github.com/mbhall88/drprg>. We used commit 9492f25 for all results
64 via a Singularity[1] container from the URI
65 `docker://quay.io/mbhall88/drprg:9492f25`.

66 All code used to generate results for this study are available on GitHub at
67 <https://github.com/mbhall88/drprg-paper>. All data used in this work are freely available from
68 the SRA/ENA/DRA and a copy of the datasheet with all associated phenotype information
69 can be downloaded from the archived repository at <https://doi.org/10.5281/zenodo.7819984>
70 or found in the previously mentioned GitHub repository.

71 The *Mycobacterium tuberculosis* index used in this work is available to download through
72 DrPRG via the command `drprg index --download mtb@20230308` or from
73 GitHub at <https://github.com/mbhall88/drprg-index>.

74 5. Introduction

75 Human industrialisation of antibiotic production and use over the last 100 years has led to a
76 global rise in prevalence of antibiotic resistant bacterial strains. The phenomenon
77 was even observed within patients in the first clinical trial of streptomycin as a drug for
78 tuberculosis (TB) in 1948[2], and indeed as every new drug class has been introduced, so has
79 resistance followed. Resistance mechanisms are varied, and can be caused by point mutations
80 at key loci (e.g., binding sites of drugs[3,4]), frame-shifts rendering a gene non-functional[5],
81 horizontal acquisition of new functionality via a new gene[6], or by up-regulation of efflux
82 pumps to reduce the drug concentration within the cell[7].
83

84 Phenotypic and genotypic methods for detecting reduced susceptibility to drugs play
85 complementary roles in clinical microbiology. Carefully defined phenotypic assays are used
86 to give (semi)quantitative or binary measures of drug susceptibility; these have the benefit of

87 being experimental, quantitative measurements, and are able to detect resistance caused by
88 hitherto unknown mechanisms. Prediction of drug resistance from genomic data has different
89 advantages. Detection of a single nucleotide polymorphism (SNP) is arguably more
90 consistent than a phenotypic assay, as it is not affected by whether the resistance it causes is
91 near some threshold defining a resistant/susceptible boundary. Additionally, combining
92 sequence datasets from different labs is more reliable than combining different phenotypic
93 datasets, and using sequence data allows one to detect informative genetic changes (e.g., a
94 tandem expansion of a single gene to form an array, thus increasing dosage). More subtly,
95 defining the cut-off to separate resistant from susceptible is only simple when the minimum
96 inhibitory concentration distribution is a simple bimodal distribution; in reality it is
97 sometimes a convolution of multiple distributions caused by different mutations, and genetic
98 data is sometimes needed to deconvolve the data and choose a threshold[8,9].
99

100 The key requirement for a genomic predictor is to have an encodable understanding of the
101 genotype-to-phenotype map. Research has focussed on clinically important pathogens,
102 primarily *Escherichia coli*, *Klebsiella pneumoniae*, *Salmonella enterica*, *Pseudomonas*
103 *aeruginosa* and *Mycobacterium tuberculosis* (MTB). The challenges differ across species;
104 almost all bacterial species are extremely diverse, with non-trivial pan-genomes and
105 considerable horizontal gene transfer causing transmission of resistance genes[10]. In these
106 cases, species are so diverse that detection of chromosomal SNPs is affected heavily by
107 reference bias[11]. Furthermore, there is an appreciable proportion of resistance which is not
108 currently explainable through known SNPs or genes [12–14]. At the other extreme, MTB has
109 almost no accessory genome, and no recombination or plasmids[15]. Resistance appears to be
110 caused entirely by mutations, indels, and rare structural variants, and simple sets of rules ("if
111 any of these mutations are present, or any of these genes inactivated, the sample is resistant")
112 work well for most drugs[16]. MTB has an exceptionally slow growth rate, meaning culture-
113 based drug susceptibility testing (DST) is slow (2-4 weeks depending on media), and
114 therefore sequencing is faster[17]. As part of the end TB strategy, the WHO strives towards
115 universal access to DST[18], defining Target Product Profiles for molecular
116 diagnostics[19,20] and publishing a catalogue of high-confidence resistance mutations
117 intended to provide a basis for commercial diagnostics and future research[16]. There was a
118 strong community-wide desire to integrate this catalogue into software for genotypic
119 resistance prediction, although independent benchmarking confirmed there was still need for
120 improvement[12]. Hence, there is a continuing need to improve the understanding of the
121 genetic basis of resistance and integrate it into software for genotypic DST.
122

123 In this paper we develop and evaluate a new software tool for genotypic DST for MTB, built
124 on a generic framework that can be used for any bacteria. Several tools have been developed
125 previously[21–25]. Of these, only Mykrobe and TBProfiler work on Illumina and Nanopore
126 data, and both have been heavily evaluated previously[22,23,26,27] - so we benchmark
127 against these. Mykrobe uses de Bruijn graphs to encode known resistance alleles and thereby
128 achieves high accuracy even on indel calls with Nanopore data[27]. However it is unable to
129 detect novel alleles in known resistance genes, nor to detect gene truncation or deletion,
130 which would be desirable. TBProfiler is based on mapping and variant calling (by default
131 using Freebayes[28]), and detects gene deletions using Delly[29].
132

133 Our new software, called DrPRG (Drug resistance Prediction with Reference Graphs), builds
134 on newer pan-genome technology than Mykrobe[11] using an independent graph for each
135 gene in the catalogue, which makes it easier to go back-and-forth between VCF and the

136 graph. To build an index, it takes as input a catalogue of resistant variants (a simple 4-column
137 TSV file), a file specifying expert rules (e.g. any missense variant between codons X and Y in
138 gene Z causes resistance to drug W), and a VCF of population variation in the genes of
139 interest. This allows it to easily incorporate the current WHO-endorsed catalogue[16], which
140 is conservative, and for the user to update the catalogue or rules with minimal effort. Finally,
141 to provide resistance predictions, it takes a prebuilt index (an MTB one is currently provided)
142 and sequencing reads (FASTQ).

143
144 We describe the DrPRG method, and to evaluate it, gather the largest MTB dataset of
145 sequencing data with associated phenotype information and reveal novel insights into
146 resistance-determining mutations for this species.

147 **6. Methods**

148 DrPRG is a command-line software tool implemented in the Rust programming language.
149 There are two main subcommands: `build` for building a reference graph and associated
150 index files, and `predict` for producing genotypic resistance predictions from sequencing
151 reads and an index (from `build`).

152 **6.1 Constructing a resistance-specific reference graph and index**

153 The `build` subcommand of DrPRG requires a Variant Call Format (VCF) file of variants
154 from which to build a reference graph, a catalogue of mutations that confer resistance or
155 susceptibility for one or more drugs, and an annotation (GFF) and FASTA file of the
156 reference genome.

157 For this work, we used the reference and annotation for the MTB strain H37Rv (accession
158 NC_000962.3) and the default mutation catalogue from Mykrobe (v0.12.1)[12,26].
159 To ensure the reference graph is not biased towards a particular lineage or susceptibility
160 profile, we selected samples from a VCF of 15,211 global MTB samples[30]. We randomly
161 chose 20 samples from each lineage 1 through 4, as well as 20 samples from all other
162 lineages combined. In addition, we included 17 clinical samples representing MTB global
163 diversity (lineages 1-6)[31,32] to give a total of 117 samples. In the development phase of
164 DrPRG we also found it necessary to add some common mutations not present in these 177
165 samples; as such, we added 48 mutations to the global VCF (these mutations are listed in
166 archived repository – see Data summary). We did not add all catalogue mutations as there is a
167 saturation point for mutation addition to a reference graph, and beyond this point,
168 performance begins to decay[33].

169 The `build` subcommand turns this VCF into a reference graph by extracting a consensus
170 sequence for each gene and sample. We use just those genes that occur in the mutation
171 catalogue and include 100 bases flanking the gene. A multiple sequence alignment is
172 constructed for each gene from these consensus sequences with MAFFT (v7.505)[34,35] and
173 then a reference graph is constructed from these alignments with `make_prg` (v0.4.0)[11].
174 The final reference graph is then indexed with `pandora`[11].

175 **6.2 Genotypic resistance prediction**

176 Genotypic resistance prediction of a sample is performed by the `predict` subcommand of
177 DrPRG. It takes an index produced by the `build` command (see [Constructing a resistance-
178 specific reference graph and index](#)) and sequencing reads – Illumina or Nanopore are
179 accepted. To generate predictions, DrPRG discovers novel variants (`pandora`), adds these to
180 the reference graph (`make_prg` and MAFFT), and then genotypes the sample with respect

181 to this updated graph (*pandora*). The genotyped VCF is filtered such that we ignore any
182 variant with less than 3 reads supporting it and require a minimum of 1% read depth on each
183 strand. Next, each variant is compared to the catalogue. If an alternate allele has been called
184 that corresponds with a catalogue variant, resistance ('R') is noted for the drug(s) associated
185 with that mutation. If a variant in the VCF matches a catalogue mutation, but the genotype is
186 null ('.'), we mark that mutation, and its associated drug(s), as failed ('F'). Where an alternate
187 allele call does not match a mutation in the catalogue, we produce an unknown ('U')
188 prediction for the drug(s) that have a known resistance-conferring mutation in the relevant
189 gene.

190 DrPRG also has the capacity to detect minor alleles and call minor resistance ('r') or minor
191 unknown ('u') in such cases. Minor alleles are called when a variant (that has passed the
192 above filtering) is genotyped as being the susceptible (reference) allele, but there is also read
193 depth on the resistant (alternate) allele above a given minor allele frequency parameter (--
194 *maf*; default is 0.1 for Illumina data). Minor allele calling is turned off by default for
195 Nanopore data as we found it led to a drastic increase in the number of false positive calls
196 (this is also the case for Mykrobe and TBProfiler).

197 When building the index for DrPRG and making predictions, we also accept a file of "expert
198 rules" for calling variants of a certain class. A rule is associated with a gene, an optional
199 position range, a variant type, and the drug(s) that rule confers resistance to. Currently
200 supported variant types are missense, nonsense, frameshift, and gene absence.

201 The output of running predict is a VCF file of all variants in the graph and a JSON file of
202 resistance predictions for each drug in the index, along with the mutation(s) supporting that
203 prediction and a unique identifier to find that variant in the VCF file (see Supplementary
204 Section S1 for an example). The reference graph gene presence/absence (as determined by
205 *pandora*) is also listed in the JSON file.

206 6.3 Benchmark

207 We compare the performance of DrPRG against Mykrobe (v0.12.1)[26] and TBProfiler
208 (v4.3.0)[22] for MTB drug resistance prediction. Mykrobe is effectively a predecessor of
209 DrPRG; it uses genome graphs, in the form of de Bruijn graphs, to construct a graph of all
210 mutations in a catalogue and then genotypes the reads against this graph. TBProfiler is a more
211 traditional approach which aligns reads to a single reference genome and calls variants from
212 that via aligned haplotype sequences.

213 A key part of such a benchmark is the catalogue of mutations, as this generally accounts for
214 the majority of differences between tools[26]. As such, we use the same catalogue for all
215 tools to ensure any differences are method-related - not catalogue disparities. The catalogue
216 we chose is the default one provided in Mykrobe[12]. It is a combination of the catalogue
217 described in Hunt *et al.* [26] and the category 1 and 2 mutation and expert rules from the
218 2021 WHO catalogue[16]. This catalogue contains mutations for 14 drugs: isoniazid,
219 rifampicin, ethambutol, pyrazinamide, levofloxacin, moxifloxacin, ofloxacin, amikacin,
220 capreomycin, kanamycin, streptomycin, ethionamide, linezolid, and delamanid.

221 We used Mykrobe and TBProfiler with default parameters, except for a parameter in each
222 indicating the sequencing technology of the data as Illumina or Nanopore and the TBProfiler
223 option to not trim data (as we do this in [Quality control](#)).

224 We compare the prediction performance of each program using sensitivity and specificity. To
225 calculate these metrics, we consider a true positive (TP) and true negative (TN) as a case
226 where a program calls resistance and susceptible, respectively, and the phenotype agrees; a
227 false positive (FP) as a resistant call by a program but a susceptible phenotype, with false

228 negatives (FN) being the inverse of FP. We only present results for drugs in the catalogue and
229 where at least 10 samples had phenotypic data available.

230 To benchmark the runtime and memory usage of each tool, we used the Snakemake
231 benchmark feature within our analysis pipeline[36].

232 **6.4 Datasets**

233 We gathered various MTB datasets where whole-genome sequencing data (Nanopore or
234 Illumina) were available from public repositories (ENA/SRA/DRA) and associated
235 phenotypes were accessible for at least one drug present in our catalogue[16,27,37–49].
236 All data was downloaded with `fastq-dl` (v1.1.1; <https://github.com/rpetit3/fastq-dl>).

237 **6.5 Quality control**

238 All downloaded Nanopore fastq files had adapters trimmed with `porechop` (v0.2.4;
239 <https://github.com/rwick/Porechop>), with the option to discard any reads with an adapter in
240 the middle, and any reads with an average quality score below 7 were removed with `nanoq`
241 (v0.9.0)[50]. Illumina reads were pre-processed with `fastp` (v0.23.2)[51] to remove adapter
242 sequences, trim low quality bases from the ends of the reads, and remove duplicate reads and
243 reads shorter than 30bp.

244 Sequencing reads were decontaminated as described in Hall *et al.*[27] and Walker *et al.*[16].
245 Briefly, sequenced reads were mapped to a database of common sputum contaminants and the
246 MTB reference genome (H37Rv; accession NC_000962.3)[52] keeping only those reads
247 where the best mapping was to H37Rv.

248 After quality control, we removed any sample with average read depth less than 15, or where
249 more than 5% of the reads mapped to contaminants.

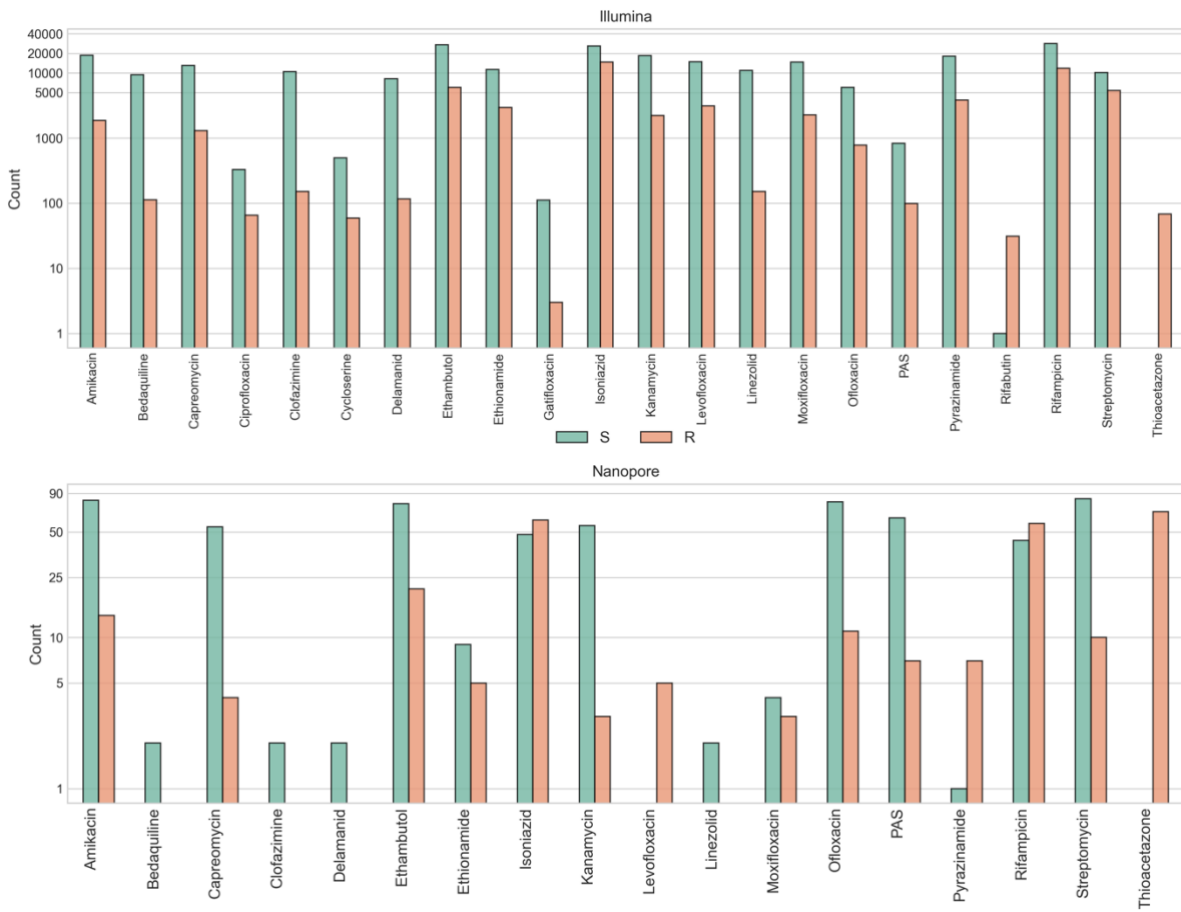
250 Lineage information was extracted from the TBProfiler results (see [Benchmark](#)).

251 **6.6 Statistical Analysis**

252 We used a Wilcoxon rank-sum paired data test from the Python library SciPy[53] to test for
253 significant differences in runtime and memory usage between the three prediction tools.
254 The sensitivity and specificity confidence intervals were calculated with a Wilson's score
255 interval with a coverage probability of 95%.

256 **7. Results**

257 To benchmark DrPRG, Mykrobe, and TBProfiler, we gathered an Illumina dataset of 45,702
258 MTB samples with a phenotype for at least one drug. After quality control (see [Quality](#)
259 [control](#)), this number reduced to 44,709. In addition, we gathered 142 Nanopore samples, of
260 which 138 passed quality control. In Figure 1 we show all available drug phenotypes for
261 those interested in the dataset, yet our catalogue does not offer predictions for all drugs listed
262 (see [Benchmark](#)). Lineage counts for all samples that passed quality control and have a
263 single, major lineage call can be found in Table 1.



264
265 **Figure 1: Drug phenotype counts for Illumina (upper) and Nanopore (lower) datasets. Bars are stratified and**
266 **267 coloured by whether the phenotype is resistant (R; orange) or susceptible (S; green). Note, the y-axis is log-scaled.**
PAS=para-aminosalicylic acid

268 **Table 1: Lineage counts from the Illumina and Nanopore datasets, covering main lineages 1-9 (L1-L9) and the three**
269 **livestock-associated lineages (La1-La3) as defined in [54]**

Lineage	Illumina	Nanopore
La1	239	0
La2	7	0
La3	71	0
L1	3907	32
L2	12870	38
L3	5803	9
L4	20731	59
L5	63	0
L6	78	0
L7	3	0
L9	1	0

270
271 **7.1 Sensitivity and specificity performance**

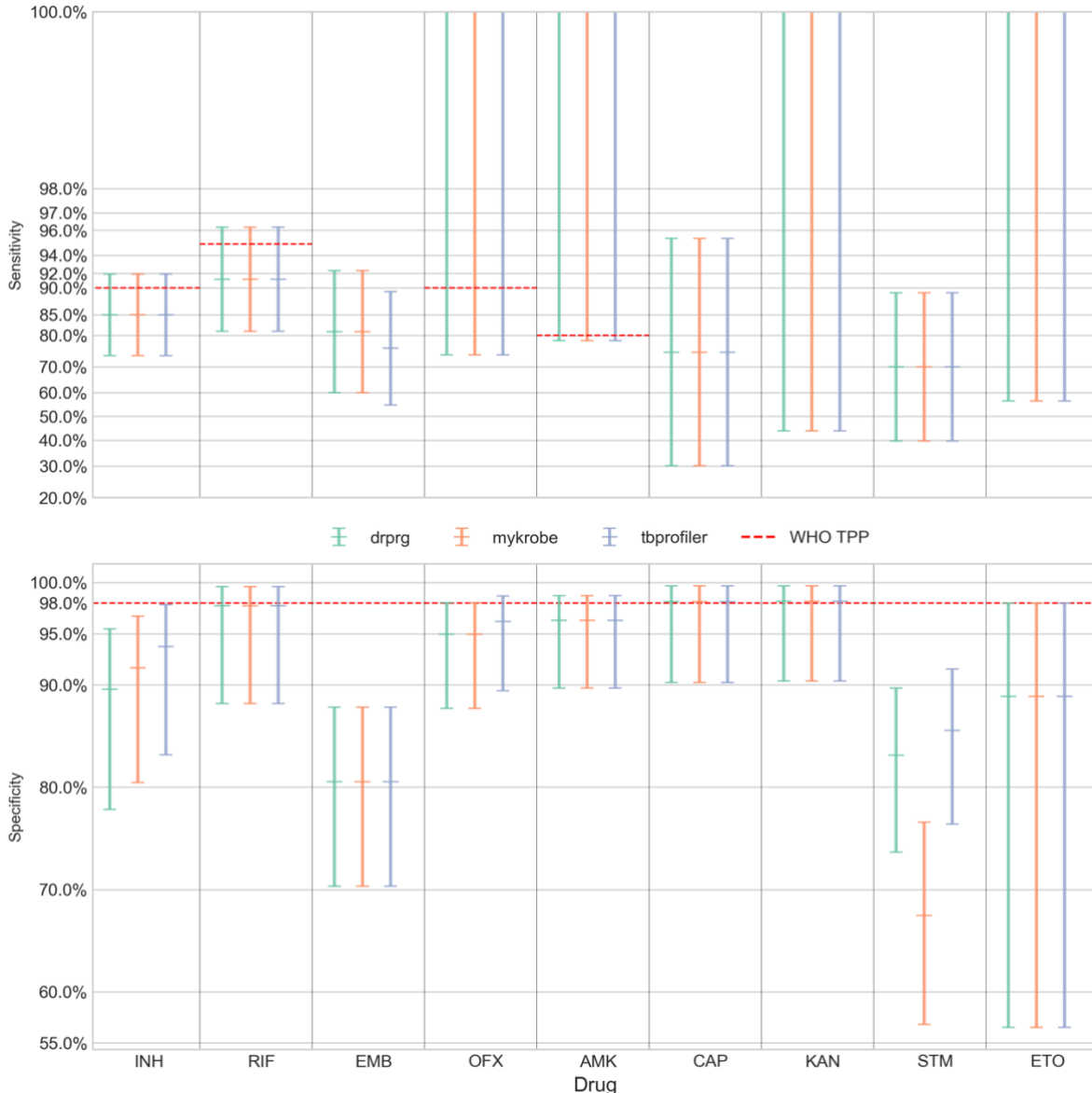
272 We present the sensitivity and specificity results for Illumina data in Figure 2 and Suppl.
273 Table S1 and the Nanopore data in Figure 3 and Suppl. Table S2.

274 When comparing DrPRG's performance to that of Mykrobe and TBProfiler, we look for
275 instances where the confidence intervals do not overlap; indicating a significant difference.
276 With Illumina data (Figure 2 and Suppl. Table S1), DrPRG achieves significantly greater
277 sensitivity than Mykrobe for rifampicin (96.4% [96.0-96.7] vs. 95.6% [95.2-95.9]),
278 streptomycin (85.3% [84.4-86.3] vs. 83.1% [82.1-84.1]), amikacin (85.6% [83.9-87.1] vs.
279 80.8% [78.9-82.5]), capreomycin (77.5% [75.2-79.7] vs. 71.8% [69.3-74.1]), kanamycin
280 (83.7% [82.1-85.2] vs. 79.9% [78.2-81.5]), and ethionamide (75.2% [73.7-76.8] vs. 71.4%
281 [69.7-73.0]), with no significant difference for all other drugs. In terms of sensitivity, there
282 was no significant difference between DrPRG and TBProfiler except for ethionamide, where
283 DrPRG was significantly more sensitive (75.2% [73.7-76.8] vs. 71.5% [69.8-73.1]). For
284 specificity, there was no significant difference between the tools except that DrPRG and
285 Mykrobe were significantly better than TBProfiler for rifampicin (97.8% [97.6-98.0] vs.
286 97.2% [97.0-97.4]). There was no significant difference in sensitivity or specificity for any
287 drug with Nanopore data.



288
289
290
291
292 **Figure 2: Sensitivity (upper panel; y-axis) and specificity (lower panel; y-axis) of resistance predictions for different**
293 **drugs (x-axis) from Illumina data. Error bars are coloured by prediction tool. The central horizontal line in each**
294 **error bar is the sensitivity/specificity and the error bars represent the 95% confidence interval. Note, the sensitivity**
295 **panel's y-axis is logit-scaled. This scale is similar to a log scale close to zero and to one (100%), and almost linear**

293 around 0.5 (50%). The red dashed line in each panel represents the minimal standard WHO target product profile
294 (TPP; where available) for next-generation drug susceptibility testing for sensitivity and specificity. INH=isoniazid,
295 RIF=rifampicin, EMB=ethambutol, PZA=pyrazinamide, LFX=levofloxacin, MFX=moxifloxacin, OFX=ofloxacin,
296 AMK=amikacin, CAP=capreomycin, KAN=kanamycin, STM=streptomycin, ETO=ethionamide, LZD=linezolid,
297 DLM=delamanid.



298
299 **Figure 3: Sensitivity (upper panel; y-axis) and specificity (lower panel; y-axis) of resistance predictions for different**
300 **drugs (x-axis) from Nanopore data. Error bars are coloured by prediction tool. The central horizontal line in each**
301 **error bar is the sensitivity/specificity and the error bars represent the 95% confidence interval. Note, the sensitivity**
302 **panel's y-axis is logit-scaled. This scale is similar to a log scale close to zero and to one (100%), and almost linear**
303 **around 0.5 (50%). The red dashed line in each panel represents the minimal standard WHO target product profile**
304 **(TPP; where available) for next-generation drug susceptibility testing for sensitivity and specificity. INH=isoniazid,**
305 **RIF=rifampicin, EMB=ethambutol, OFX=ofloxacin, AMK=amikacin, CAP=capreomycin, KAN=kanamycin,**
306 **STM=streptomycin, ETO=ethionamide.**

307 In both figures, we show the minimal requirements from the WHO target product profiles for
308 sensitivity and specificity of genotypic drug susceptibility testing[19] as red dashed lines.
309 Note, a sensitivity target is not specified by the WHO for ethambutol (EMB), capreomycin
310 (CAP), kanamycin (KAN), streptomycin (STM), or ethionamide (ETO). For Illumina data, all
311 tools' predictions for rifampicin, isoniazid, levofloxacin, moxifloxacin and amikacin are

312 above the sensitivity minimal requirement target. TBProfiler also exceeds the target for
313 pyrazinamide, which DrPRG misses by 0.2%. No drug's sensitivity target was achieved with
314 Nanopore data. For specificity, the tools are all very similar and either exceed or fall below
315 the threshold together (see Figure 2). The target of >98% is met by all tools on Illumina data
316 only for ofloxacin, amikacin, linezolid, and delamanid. Mykrobe also exceeds the target for
317 capreomycin. As such, amikacin is the only drug where both sensitivity and specificity
318 performance exceed the minimal requirement of the WHO target product profiles. Only
319 capreomycin and kanamycin specificity targets are exceeded (by all tools) with Nanopore
320 data.

321 However, for Illumina data, we did find that likely sample-swaps or phenotype instability[55]
322 could lead to some drugs being on the threshold of the WHO target product profiles. If we
323 excluded samples where all three tools make a FP call for the strong isoniazid and rifampicin
324 resistance-conferring mutations *katG* S315T ($n=152$) and *rpoB* S450L ($n=119$) [16]
325 respectively, all three tools would exceed the isoniazid specificity target of 98% - thus
326 meeting both sensitivity and specificity targets for isoniazid. In addition, DrPRG and
327 Mykrobe would meet the rifampicin specificity target of 98% - leading to both targets being
328 met for rifampicin for these two tools. As previously reported [55,56], we also found a lot of
329 instability in the ethambutol result caused by *embB* mutations M306I ($n=827$) and M306V
330 ($n=519$) being called for phenotypically susceptible samples (FP) by all three tools. Other
331 frequent consensus FP calls included: *fabG1* c-15t, which is associated with ethionamide
332 ($n=441$) and isoniazid ($n=241$) resistance; *rrs* a1401g, which is associated with resistance to
333 capreomycin ($n=241$), amikacin ($n=70$), and kanamycin ($n=48$). In addition there were
334 common false positives from *gyrA* mutations A90V and D94G, which are associated with
335 resistance to the fluoroquinolones levofloxacin ($n=108$ and $n=70$, respectively), moxifloxacin
336 ($n=419$ and $n=349$) and ofloxacin ($n=19$ and $n=17$), and are known to cause heteroresistance
337 and minimum inhibitory concentrations (MIC) close to the critical concentration
338 threshold[57-59].

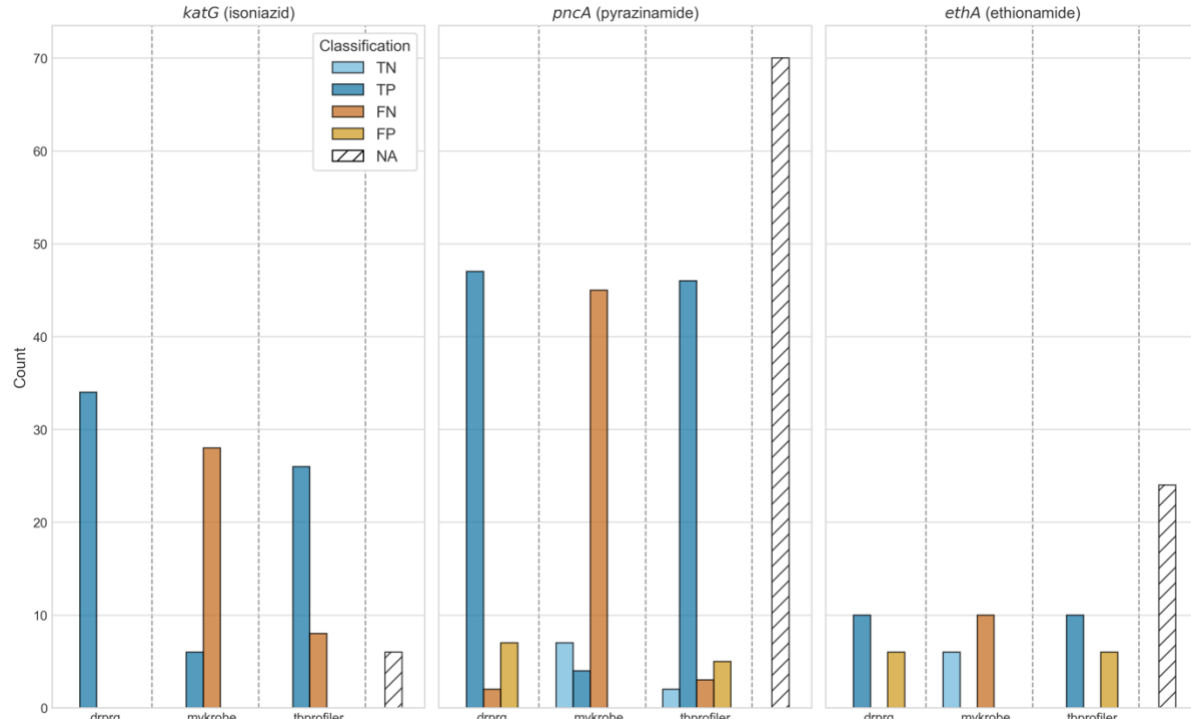
339 7.2 Evaluation of potential additions to the WHO catalogue

340 False negatives are much harder to investigate as it is not known which mutation(s) were
341 missed as they are presumably not in the catalogue if all tools failed to make a call. However,
342 looking through those FNs where DrPRG makes an "unknown" resistance call, we note some
343 potential mutations that may need reclassification or inclusion in the WHO catalogue. For
344 delamanid FNs, we found five different nonsense mutations in the *ddn* gene in seven samples
345 – W20* ($n=2$), W27* ($n=1$), Q58* ($n=1$), W88* ($n=2$), and W139* ($n=1$) – none of which
346 occurred in susceptible samples. We also found 13 pyrazinamide FN cases with a nonstop
347 (stop-loss) mutation in *pncA* – this mutation type was also seen in two susceptible samples.
348 Another *pncA* mutation, T100P, was also observed in 10 pyrazinamide FN samples and no
349 susceptible samples. T100P only appears once in the WHO catalogue data ("solo" in a
350 resistant sample). As such, it was given a grading of uncertain significance. As our dataset
351 includes those samples in the WHO catalogue dataset, this means an additional nine isolates
352 have been found with this mutation - indicating this may warrant an upgrade to 'associated
353 with resistance'. We found an interesting case of allele combinations, where nine ethambutol
354 FN samples have the same two *embA* mutation c-12a and c-11a and *embB* mutation P397T -
355 this combination is only seen in two susceptible samples. Interestingly, *embB* P397T and
356 *embA* c-12a don't appear in the WHO catalogue, but have been described as causing
357 resistance previously[60]. Three *katG* mutations were also detected in isoniazid FN cases.
358 First, G279D occurs in eight missed resistance samples and no susceptible cases. This
359 mutation is graded as 'uncertain significance' in the WHO catalogue and was seen solo in

360 four resistant samples in that data. Singh *et al.* performed a protein structural analysis caused
361 by this mutation and found it produced “an undesirable effect on the functionality of the
362 protein”[61]. Second, G699E occurs in eight FN samples and no susceptible cases, but has a
363 WHO grading of ‘uncertain significance’ based on six resistant isolates; thus, we add two
364 extra samples to that count. And third, N138H occurs in 14 FN samples and one susceptible.
365 In seven of these cases, it co-occurs with *ahpC* mutations t-75g ($n=2$) and t-76a ($n=5$). This
366 mutation occurs in only three resistant isolates in the WHO catalogue dataset, giving it an
367 uncertain significance, but we add a further 11 cases. This mutation has been found to cause a
368 high isoniazid MIC and be associated with resistance[62,63].

369 7.3 Detection of large deletions

370 There are expert rules in the WHO catalogue which treat gene loss-of-function (any
371 frameshift or nonsense mutation) in *katG*, *ethA*, *gid*, and *pncA* as causing resistance for
372 isoniazid, ethionamide, streptomycin, and pyrazinamide, respectively[16]. Although
373 examples of resistance caused by gene deletion are rare[64–68], with a dataset of this size
374 ($n=44,709$), we can both evaluate these rules, and compare the detection power of DrPRG
375 and TBProfiler for identifying gene deletions (Mykrobe does not, although in principle it
376 could). In total we found 206 samples where DrPRG and/or TBProfiler identified deletions of
377 *ethA*, *katG*, or *pncA*. Although many of these isolates did not have phenotype information for
378 the associated drug ($n=100$), the results are nevertheless striking (Figure 4). Given the low
379 false-positive rate of pandora for gene absence detection[11], these no-phenotype samples
380 provide insight into how often gene deletions are occurring in clinical samples.
381 Of the 34 isolates where *katG* was identified as being absent, and an isoniazid phenotype was
382 available, all 34 were phenotypically resistant. DrPRG detected all 34 (100% sensitivity) and
383 TBProfiler identified 26 (76.5% sensitivity). Deletions of *pncA* were detected in 56 isolates,
384 of which 49 were phenotypically resistant. DrPRG detected 47 (95.9% sensitivity) and
385 TBProfiler detected 46 (93.9% sensitivity). Lastly, *ethA* was found to be missing in 16
386 samples with an ethionamide phenotype, of which 10 were phenotypically resistant. Both
387 DrPRG and TBProfiler correctly predicted all 10 (100% sensitivity). No *gid* deletions were
388 discovered. We note that the TP calls made by Mykrobe were due to it detecting large
389 deletions that are present in the catalogue, which is understandable given the whole gene is
390 deleted.
391 We conclude that DrPRG is slightly more sensitive at detecting large deletions than
392 TBProfiler (and Mykrobe) for *katG*, and equivalent for *pncA* and *ethA*. However we note that
393 the WHO expert rule which predicts resistance to isolates missing specific genes appears
394 more accurate for *katG* (100% of isolates missing the gene are resistant) than for *pncA* (87%
395 resistant) and *ethA* (62.5% resistant).



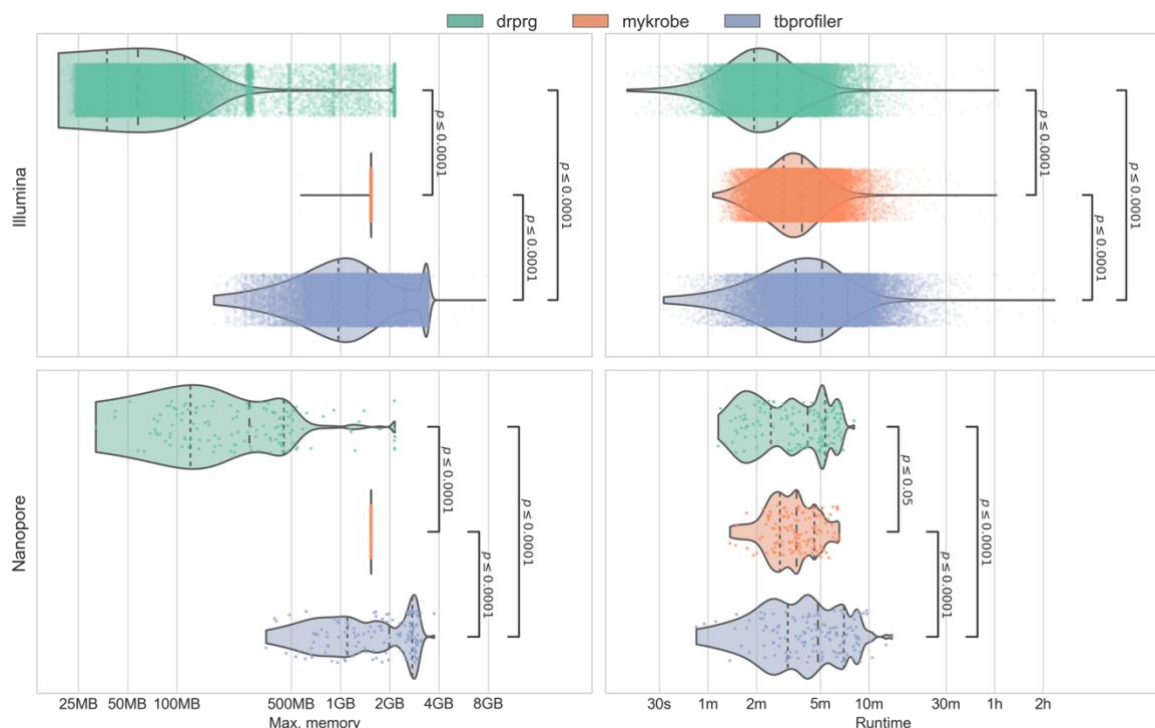
396
397
398
399
400
401

Figure 4: Impact of gene deletion on resistance classification. The title of each subplot indicates the gene and drug it effects. Bars are coloured by their classification and stratified by tool. Count (y-axis) indicates the number of gene deletions for that category. The NA bar (white with diagonal lines) indicates the number of samples with that gene deleted but no phenotype information for the respective drug. TP=true positive; FN=false negative; TN=true negative; FP=false positive; NA=no phenotype available.

402
403
404
405
406
407
408
409
410
411

7.4 Runtime and memory usage benchmark

The runtime and peak memory usage of each program was recorded for each sample and is presented in Figure 5. DrPRG (median 161 seconds) was significantly faster than both TBProfiler (307 seconds; $p \leq 0.0001$) and Mykrobe (230 seconds; $p \leq 0.0001$) on Illumina data. For Nanopore data, DrPRG (250 seconds) was significantly faster than TBProfiler (290 seconds; $p \leq 0.0001$), but significantly slower than Mykrobe (213 seconds; $p = 0.0347$). In terms of peak memory usage, DrPRG (Illumina median peak memory 58MB; Nanopore 277MB) used significantly less memory than Mykrobe (1538MB; 1538MB) and TBProfiler (1463MB; 1990MB) on both Illumina and Nanopore data ($p \leq 0.0001$ for all comparisons).



412
413 **Figure 5: Benchmark of the maximum memory usage (left panels) and runtime (right panels) from Illumina (upper**
414 **row) and Nanopore (lower row) data. Each point and violin is coloured by the tool, with each point representing a**
415 **single sample. Statistical annotations are the result of a Wilcoxon rank-sum paired data test on each pair of tools.**
416 **Dashed lines inside the violins represent the quartiles of the distribution. Note, the x-axis is log-scaled.**

8. Discussion

418 In this work, we have presented a novel method for making drug resistance predictions with
419 reference graphs. The method, DrPRG, requires only a reference genome and annotation, a
420 catalogue of resistance-conferring mutations, a VCF of population variation from which to
421 build a reference graph, and (optionally) a set of rules for types of variants in specific genes
422 which cause resistance. We apply DrPRG to the pathogen *M. tuberculosis*, for which there is
423 a great deal of information on the genotype/phenotype relationship, and a great need to
424 provide good tools which implement and augment current and forthcoming versions of the
425 WHO catalogue. We illustrate the performance of DrPRG against two existing methods for
426 drug resistance prediction – Mykrobe and TBProfiler.

427 We benchmarked the methods on a high-quality Illumina sequencing dataset with associated
428 phenotype profiles for 44,709 MTB genomes; the largest known dataset to-date[16]. All tools
429 used the same catalogue and rules, and for most drugs, there was no significant difference
430 between the tools. However, DrPRG did have a significantly higher specificity than
431 TBProfiler for rifampicin predictions, and sensitivity for ethionamide predictions. DrPRG's
432 sensitivity was also significantly greater than Mykrobe's for rifampicin, streptomycin,
433 amikacin, capreomycin, kanamycin, and ethionamide. Evaluating detection of gene loss, we
434 found DrPRG was more sensitive to *katG* deletions than TBProfiler.

435 We also benchmarked using 138 Nanopore-sequenced MTB samples with phenotype
436 information, but found no significant difference between the tools. This Nanopore dataset
437 was quite small and therefore the confidence intervals were large for all drugs. Increased
438 Nanopore sequencing over time will provide better resolution of the overall sensitivity and
439 specificity values and improve the methodological nuances of calling variants from this
440 emerging, and continually changing, sequencing technology.

442 DrPRG also used significantly less memory than Mykrobe and TBProfiler on both Nanopore
443 and Illumina data. In addition, the runtime of DrPRG was significant faster than both tools on
444 Illumina data and faster than TBProfiler on Nanopore data. While the absolute values for
445 memory and runtime for all tools mean they could all easily run on common computers found
446 in the types of institutions likely to run them, the differences for the Nanopore data warrant
447 noting. As Nanopore data can be generated “in the field”, computational resource usage is
448 critical. For example, in a recent collaboration of ours with the National Tuberculosis
449 program in Madagascar[27], Nanopore sequencing and analysis are regularly performed on a
450 laptop, meaning memory usage is sometimes a limiting factor. DrPRG’s median peak
451 memory was 277MB, meaning it can comfortably be run on any laptop and other mobile
452 computing devices[69].

453 It is clear from the Illumina results that more work is needed to understand resistance-
454 conferring mutations for delamanid and linezolid. However, we did find that nonsense
455 mutations in the *ddn* gene appear likely to be resistance-conferring for delamanid – as has
456 been noted previously[39,70–72]. We also found a novel (likely) mechanism of resistance to
457 pyrazinamide - a nonstop mutation in *pncA*. Phenotype instability in *embB* at codon 306 was
458 also found to be the main driver in poor ethambutol specificity, as has been noted
459 elsewhere[55,56], indicating the need to further investigate cofactors that may influence the
460 phenotype when mutations at this codon are present.

461 Gene absence/deletion detection allowed us to confirm that the absence of *katG* – a
462 mechanism which is rare in clinical samples[64–67,73] - is highly likely to confer resistance
463 to isoniazid. Additionally, we found that the absence of *pncA* is likely to cause resistance to
464 pyrazinamide, as has been noted previously[68]. One finding that requires further
465 investigation is the variability in ethionamide phenotype when *ethA* is absent. We found that
466 only 63% of the samples with *ethA* missing, and an ethionamide phenotype, were resistant.
467 An *et al.* have suggested that *ethA* deletion alone does not always cause resistance and there
468 might be an alternate pathway via *mshA*[74].

469 Given the size of the Illumina dataset used in this work, the results provide a good marker of
470 Illumina whole-genome sequencing’s ability to replace traditional phenotyping methods.
471 With the catalogue used in this study, DrPRG meets the WHO’s target product profile for
472 next-generation drug-susceptibility testing for both sensitivity and specificity for amikacin,
473 and sensitivity only for rifampicin, isoniazid, levofloxacin, and moxifloxacin. However, if we
474 exclude cases where all tools call *rpoB* S450L or *katG* S315T for phenotypically susceptible
475 samples (these are strong markers of resistance[16] and therefore we suspect sample-swaps or
476 phenotype error[75]), DrPRG also meets the specificity target product profile for rifampicin
477 and isoniazid. For the other first-line drugs ethambutol and pyrazinamide, ethambutol does
478 not have a WHO target and DrPRG’s sensitivity is 0.2% below the WHO target (although the
479 confidence interval spans the target), while the specificity target is missed by 0.8%.

480 The primary limitation of the DrPRG method relates to minor allele calls. DrPRG uses
481 *pandora* for novel variant discovery, which combines a graph of known population variants
482 (which can be detected at low frequency) with *de novo* detection of other variants if present at
483 above ~50% frequency. Thus, it can miss minor allele calls if the allele is absent from its
484 reference graph. While this issue did not impact most drugs, it did account for the majority of
485 cases where DrPRG missed pyrazinamide-resistant calls (in *pncA*), but the other tools
486 correctly called resistance. Unlike most other genes, where there are a relatively small
487 number of resistance-conferring mutations, or they’re localised to a specific region (e.g. the
488 rifampicin-resistance determining region in *rpoB*), resistance-conferring mutations are
489 numerous - with most being rare - and distributed throughout *pncA*[16,76,77]. Adding all of
490 these mutations will, and does, lead to decreased performance of the reference graph[33], and

491 so improving minor allele calling for pyrazinamide remains a challenge we need to revisit in
492 the future.

493 One final limitation is the small number of Nanopore-sequenced MTB isolates with
494 phenotypic information. In order to get a clearer picture of the sensitivities and specificities
495 this sequencing technology can provide, we need much larger and more diverse data.
496

497 In conclusion, DrPRG is a fast, memory frugal software program that can be applied to any
498 bacterial species. We showed that on MTB, it performs as well as, or better than two other
499 commonly used tools for resistance prediction. We also collected and curated the largest
500 dataset of MTB Illumina-sequenced genomes with phenotype information and hope this will
501 benefit future work to improved genotypic drug susceptibility testing for this species. While
502 we applied DrPRG to MTB in this study, it is a framework that is agnostic to the species.
503 MTB is likely one of the bacterial species with the least to gain from reference graphs given
504 its relatively conserved (closed) pan-genome compared to other common species[78]. As
505 such, we expect the benefits and performance of DrPRG to improve as the openness of the
506 species' pan-genome increases[11]; especially given its good performance on a reasonably
507 closed pan-genome.

508 9. Author statements

509 9.1 Author contributions

510 M.B.H: conceptualisation, data curation, formal analysis, investigation, methodology,
511 resources, software, visualisation, writing – original draft, writing – review & editing. L.L:
512 resources, software, writing – review & editing. L.J.M.C: funding acquisition, methodology,
513 supervision, writing – review & editing. Z.I: conceptualisation, funding acquisition,
514 methodology, supervision, writing – original draft, writing – review & editing.

515 9.2 Conflicts of interest

516 The authors declare no conflicts of interest.

517 9.3 Funding information

518 M.B.H. and L.J.M.C were supported by an Australian Government Medical Research Future
519 Fund (MRFF) grant (2020/MRF1200856).

520 9.4 Acknowledgements

521 We thank Kerri M. Malone for sharing her MTB knowledge through many discussions and
522 critiquing the final manuscript. We also thank Martin Hunt and Jeff Knaggs for facilitating
523 access to the CRyPTIC VCFs. Finally, we would like to acknowledge Timothy Walker for his
524 clinically-relevant MTB advice.

525 10. References

- 526 1. Kurtzer GM, Sochat V, Bauer MW. Singularity: Scientific containers for mobility of
527 compute. PLOS ONE. 2017;12: e0177459. doi:10.1371/journal.pone.0177459
- 528 2. Medical Research Council. Streptomycin Treatment of Pulmonary Tuberculosis: A
529 Medical Research Council Investigation. Br Med J. 1948;2: 769–782.
530 doi:10.1136/bmj.2.4582.769

531 3. Wengenack NL, Todorovic S, Yu L, Rusnak F. Evidence for Differential Binding of
532 Isoniazid by *Mycobacterium tuberculosis* KatG and the Isoniazid-Resistant Mutant
533 KatG(S315T). *Biochemistry*. 1998;37: 15825–15834. doi:10.1021/bi982023k

534 4. Hackbarth CJ, Kocagoz T, Kocagoz S, Chambers HF. Point mutations in *Staphylococcus*
535 *aureus* PBP 2 gene affect penicillin-binding kinetics and are associated with resistance.
536 *Antimicrob Agents Chemother*. 1995;39: 103–106. doi:10.1128/AAC.39.1.103

537 5. Esposito EP, Cervoni M, Bernardo M, Crivaro V, Cuccurullo S, Imperi F, et al. Molecular
538 Epidemiology and Virulence Profiles of Colistin-Resistant *Klebsiella pneumoniae* Blood
539 Isolates From the Hospital Agency “Ospedale dei Colli,” Naples, Italy. *Front Microbiol*.
540 2018;9. doi:10.3389/fmicb.2018.01463

541 6. Liu Y-Y, Wang Y, Walsh TR, Yi L-X, Zhang R, Spencer J, et al. Emergence of plasmid-
542 mediated colistin resistance mechanism MCR-1 in animals and human beings in China:
543 a microbiological and molecular biological study. *Lancet Infect Dis*. 2016;16: 161–168.
544 doi:10.1016/S1473-3099(15)00424-7

545 7. Maira-Litrán T, Allison DG, Gilbert P. An evaluation of the potential of the multiple
546 antibiotic resistance operon (mar) and the multidrug efflux pump acrAB to moderate
547 resistance towards ciprofloxacin in *Escherichia coli* biofilms. *J Antimicrob Chemother*.
548 2000;45: 789–795. doi:10.1093/jac/45.6.789

549 8. Werngren J, Sturegård E, Juréen P, Ängeby K, Hoffner S, Schön T. Reevaluation of the
550 Critical Concentration for Drug Susceptibility Testing of *Mycobacterium tuberculosis*
551 against Pyrazinamide Using Wild-Type MIC Distributions and pncA Gene Sequencing.
552 *Antimicrob Agents Chemother*. 2012;56: 1253–1257. doi:10.1128/AAC.05894-11

553 9. Schön T, Miotto P, Köser CU, Viveiros M, Böttger E, Cambau E. *Mycobacterium*
554 tuberculosis drug-resistance testing: challenges, recent developments and perspectives.
555 *Clin Microbiol Infect*. 2017;23: 154–160. doi:10.1016/j.cmi.2016.10.022

556 10. McInerney JO, McNally A, O’Connell MJ. Why prokaryotes have pangenomes. *Nat*
557 *Microbiol*. 2017;2: 17040. doi:10.1038/nmicrobiol.2017.40

558 11. Colquhoun RM, Hall MB, Lima L, Roberts LW, Malone KM, Hunt M, et al. Pandora:
559 nucleotide-resolution bacterial pan-genomics with reference graphs. *Genome Biol*.
560 2021;22: 267. doi:10.1186/s13059-021-02473-1

561 12. Hall MB, Coin LJM. Assessment of the 2021 WHO *Mycobacterium tuberculosis* drug
562 resistance mutation catalogue on an independent dataset. *Lancet Microbe*. 2022.
563 doi:10.1016/s2666-5247(22)00151-3

564 13. Mahfouz N, Ferreira I, Beisken S, von Haeseler A, Posch AE. Large-scale assessment of
565 antimicrobial resistance marker databases for genetic phenotype prediction: a systematic
566 review. *J Antimicrob Chemother*. 2020;75: 3099–3108. doi:10.1093/jac/dkaa257

567 14. Hendriksen RS, Bortolaia V, Tate H, Tyson GH, Aarestrup FM, McDermott PF. Using
568 Genomics to Track Global Antimicrobial Resistance. *Front Public Health*. 2019;7.
569 doi:10.3389/fpubh.2019.00242

570 15. Godfroid M, Dagan T, Kupczok A. Recombination Signal in *Mycobacterium tuberculosis*
571 Stems from Reference-guided Assemblies and Alignment Artefacts. *Genome Biol Evol.*
572 2018;10: 1920–1926. doi:10.1093/gbe/evy143

573 16. Walker TM, Miotto P, Köser CU, Fowler PW, Knaggs J, Iqbal Z, et al. The 2021 WHO
574 catalogue of *Mycobacterium tuberculosis* complex mutations associated with drug
575 resistance: a genotypic analysis. *Lancet Microbe.* 2022. doi:10.1016/s2666-
576 5247(21)00301-3

577 17. Votintseva AA, Bradley P, Pankhurst L, Elias C del O, Loose M, Nilgiriwala K, et al.
578 Same-Day Diagnostic and Surveillance Data for Tuberculosis via Whole-Genome
579 Sequencing of Direct Respiratory Samples. *J Clin Microbiol.* 2017;55: 1285–1298.
580 doi:10.1128/jcm.02483-16

581 18. The end TB strategy. Geneva: World Health Organization; 2015. Report No.:
582 WHO/HTM/TB/2015.19. Available: <https://www.who.int/publications/i/item/WHO->
583 HTM-TB-2015.19

584 19. Target product profile for next-generation drug-susceptibility testing at peripheral centres.
585 Geneva: World Health Organization; 2021. Available:
586 <https://www.who.int/publications/i/item/9789240032361>

587 20. MacLean EL-H, Miotto P, Angulo LG, Chiacchiarella M, Walker TM, Casenghi M, et al.
588 Updating the WHO target product profile for next-generation *Mycobacterium*
589 tuberculosis drug susceptibility testing at peripheral centres. *PLOS Glob Public Health.*
590 2023;3: e0001754. doi:10.1371/journal.pgph.0001754

591 21. Steiner A, Stucki D, Coscolla M, Borrell S, Gagneux S. KvarQ: targeted and direct
592 variant calling from fastq reads of bacterial genomes. *BMC Genomics.* 2014;15: 881.
593 doi:10.1186/1471-2164-15-881

594 22. Phelan JE, O’Sullivan DM, Machado D, Ramos J, Oppong YEA, Campino S, et al.
595 Integrating informatics tools and portable sequencing technology for rapid detection of
596 resistance to anti-tuberculous drugs. *Genome Med.* 2019;11: 41. doi:10.1186/s13073-
597 019-0650-x

598 23. Bradley P, Gordon NC, Walker TM, Dunn L, Heys S, Huang B, et al. Rapid antibiotic-
599 resistance predictions from genome sequence data for *Staphylococcus aureus* and
600 *Mycobacterium tuberculosis*. *Nat Commun.* 2015;6: 10063. doi:10.1038/ncomms10063

601 24. Kohl TA, Utpatel C, Schleusener V, Filippo MRD, Beckert P, Cirillo DM, et al. MTBseq:
602 a comprehensive pipeline for whole genome sequence analysis of *Mycobacterium*
603 tuberculosis complex isolates. *PeerJ.* 2018;6: e5895. doi:10.7717/peerj.5895

604 25. Feuerriegel S, Schleusener V, Beckert P, Kohl TA, Miotto P, Cirillo DM, et al. PhyResSE:
605 a Web Tool Delineating *Mycobacterium tuberculosis* Antibiotic Resistance and Lineage
606 from Whole-Genome Sequencing Data. *J Clin Microbiol.* 2015;53: 1908–1914.
607 doi:10.1128/JCM.00025-15

608 26. Hunt M, Bradley P, Lapierre SG, Heys S, Thomsit M, Hall MB, et al. Antibiotic
609 resistance prediction for *Mycobacterium tuberculosis* from genome sequence data with
610 Mykrobe. *Wellcome Open Res.* 2019;4: 191. doi:10.12688/wellcomeopenres.15603.1

611 27. Hall MB, Rabodoarivelos MS, Koch A, Dippenaar A, George S, Grobbelaar M, et al.
612 Evaluation of Nanopore sequencing for *Mycobacterium tuberculosis* drug susceptibility
613 testing and outbreak investigation: a genomic analysis. *Lancet Microbe.* 2022;0.
614 doi:10.1016/S2666-5247(22)00301-9

615 28. Garrison E, Marth G. Haplotype-based variant detection from short-read sequencing.
616 arXiv; 2012. doi:10.48550/arXiv.1207.3907

617 29. Rausch T, Zichner T, Schlattl A, Stütz AM, Benes V, Korbel JO. DELLY: structural
618 variant discovery by integrated paired-end and split-read analysis. *Bioinformatics.*
619 2012;28: i333–i339. doi:10.1093/bioinformatics/bts378

620 30. The CRyPTIC Consortium and the 100,000 Genomes Project. A data compendium
621 associating the genomes of 12,289 *Mycobacterium tuberculosis* isolates with
622 quantitative resistance phenotypes to 13 antibiotics. *PLOS Biol.* 2022;20: e3001721.
623 doi:10.1371/journal.pbio.3001721

624 31. Chiner-Oms Á, Berney M, Boinett C, González-Candelas F, Young DB, Gagneux S, et al.
625 Genome-wide mutational biases fuel transcriptional diversity in the *Mycobacterium*
626 tuberculosis complex. *Nat Commun.* 2019;10: 3994. doi:10.1038/s41467-019-11948-6

627 32. Letcher B, Hunt M, Iqbal Z. Gramtools enables multiscale variation analysis with
628 genome graphs. *Genome Biol.* 2021;22: 259. doi:10.1186/s13059-021-02474-0

629 33. Pritt J, Chen N-C, Langmead B. FORGe: prioritizing variants for graph genomes.
630 *Genome Biol.* 2018;19: 220. doi:10.1186/s13059-018-1595-x

631 34. Katoh K, Frith MC. Adding unaligned sequences into an existing alignment using
632 MAFFT and LAST. *Bioinformatics.* 2012;28: 3144–3146.
633 doi:10.1093/bioinformatics/bts578

634 35. Katoh K, Misawa K, Kuma K, Miyata T. MAFFT: a novel method for rapid multiple
635 sequence alignment based on fast Fourier transform. *Nucleic Acids Res.* 2002;30: 3059–
636 3066. doi:10.1093/nar/gkf436

637 36. Mölder F, Jablonski KP, Letcher B, Hall MB, Tomkins-Tinch CH, Sochat V, et al.
638 Sustainable data analysis with Snakemake. *F1000Research.* 2021;10: 33.
639 doi:10.12688/f1000research.29032.2

640 37. Gröschel MI, Owens M, Freschi L, Vargas R, Marin MG, Phelan J, et al. GenTB: A user-
641 friendly genome-based predictor for tuberculosis resistance powered by machine
642 learning. *Genome Med.* 2021;13: 138. doi:10.1186/s13073-021-00953-4

643 38. Trisakul K, Nonghanphithak D, Chaiyachat P, Kaewprasert O, Sakmongkoljitt K,
644 Reechaipichitkul W, et al. High clustering rate and genotypic drug-susceptibility
645 screening for the newly recommended anti-tuberculosis drugs among global extensively

646 drug-resistant *Mycobacterium tuberculosis* isolates. *Emerg Microbes Infect.* 2022;11:
647 1857–1866. doi:10.1080/22221751.2022.2099304

648 39. Battaglia S, Spitaleri A, Cabibbe AM, Meehan CJ, Utpatel C, Ismail N, et al.
649 Characterization of Genomic Variants Associated with Resistance to Bedaquiline and
650 Delamanid in Naive *Mycobacterium tuberculosis* Clinical Strains. *J Clin Microbiol.*
651 2020;58. doi:10.1128/jcm.01304-20

652 40. Huang H, Ding N, Yang T, Li C, Jia X, Wang G, et al. Cross-sectional Whole-genome
653 Sequencing and Epidemiological Study of Multidrug-resistant *Mycobacterium*
654 tuberculosis in China. *Clin Infect Dis Off Publ Infect Dis Soc Am.* 2019;69: 405–413.
655 doi:10.1093/cid/ciy883

656 41. Bainomugisa A, Lavu E, Hiashiri S, Majumdar S, Honjepari A, Moke R, et al. Multi-
657 clonal evolution of multi-drug-resistant/extensively drug-resistant *Mycobacterium*
658 tuberculosis in a high-prevalence setting of Papua New Guinea for over three decades.
659 *Microb Genomics.* 2018;4: e000147. doi:10.1099/mgen.0.000147

660 42. Smith C, Halse TA, Shea J, Modestil H, Fowler RC, Musser KA, et al. Assessing
661 Nanopore sequencing for clinical diagnostics: A comparison of NGS methods for
662 *Mycobacterium tuberculosis*. *J Clin Microbiol.* 2020. doi:10.1128/jcm.00583-20

663 43. Peker N, Schuele L, Kok N, Terrazos M, Neuenschwander SM, Beer J de, et al.
664 Evaluation of whole-genome sequence data analysis approaches for short- and long-read
665 sequencing of *Mycobacterium tuberculosis*. *Microb Genomics.* 2021;7.
666 doi:10.1099/mgen.0.000695

667 44. Merker M, Rasigade J-P, Barbier M, Cox H, Feuerriegel S, Kohl TA, et al.
668 Transcontinental spread and evolution of *Mycobacterium tuberculosis* W148
669 European/Russian clade toward extensively drug resistant tuberculosis. *Nat Commun.*
670 2022;13: 5105. doi:10.1038/s41467-022-32455-1

671 45. Finci I, Albertini A, Merker M, Andres S, Bablishvili N, Barilar I, et al. Investigating
672 resistance in clinical *Mycobacterium tuberculosis* complex isolates with genomic and
673 phenotypic antimicrobial susceptibility testing: a multicentre observational study.
674 *Lancet Microbe.* 2022;3: e672–e682. doi:10.1016/s2666-5247(22)00116-1

675 46. Roberts LW, Malone KM, Hunt M, Joseph L, Wintringer P, Knaggs J, et al. Repeated
676 evolution of bedaquiline resistance in *Mycobacterium tuberculosis* is driven by
677 truncation of mmpR5. *bioRxiv;* 2022. p. 2022.12.08.519610.
678 doi:10.1101/2022.12.08.519610

679 47. Di Marco F, Spitaleri A, Battaglia S, Batignani V, Cabibbe AM, Cirillo DM. Advantages
680 of long- and short-reads sequencing for the hybrid investigation of the *Mycobacterium*
681 tuberculosis genome. *Front Microbiol.* 2023;14. doi:10.3389/fmicb.2023.1104456

682 48. Lempens P, Decroo T, Aung KJM, Hossain MA, Rigouts L, Meehan CJ, et al. Initial
683 resistance to companion drugs should not be considered an exclusion criterion for the
684 shorter multidrug-resistant tuberculosis treatment regimen. *Int J Infect Dis.* 2020;100:
685 357–365. doi:10.1016/j.ijid.2020.08.042

686 49. Lempens P, Meehan CJ, Vandelannoote K, Fissette K, de Rijk P, Van Deun A, et al.
687 Isoniazid resistance levels of *Mycobacterium tuberculosis* can largely be predicted by
688 high-confidence resistance-conferring mutations. *Sci Rep.* 2018;8: 3246.
689 doi:10.1038/s41598-018-21378-x

690 50. Steinig E, Coin L. Nanoq: ultra-fast quality control for nanopore reads. *J Open Source*
691 *Softw.* 2022;7: 2991. doi:10.21105/joss.02991

692 51. Chen S, Zhou Y, Chen Y, Gu J. fastp: an ultra-fast all-in-one FASTQ preprocessor.
693 *Bioinformatics.* 2018;34: i884–i890. doi:10.1093/bioinformatics/bty560

694 52. Hunt M, Letcher B, Malone KM, Nguyen G, Hall MB, Colquhoun RM, et al. Minos:
695 variant adjudication and joint genotyping of cohorts of bacterial genomes. *Genome Biol.*
696 2022;23: 147. doi:10.1186/s13059-022-02714-x

697 53. Virtanen P, Gommers R, Oliphant TE, Haberland M, Reddy T, Cournapeau D, et al. SciPy
698 1.0: fundamental algorithms for scientific computing in Python. *Nat Methods.* 2020;17:
699 261–272. doi:10.1038/s41592-019-0686-2

700 54. Zwyer M, avusoglu C, Ghielmetti G, Pacciarini M, Scaltriti E, Van Soolingen D, et al. A
701 new nomenclature for the livestock-associated *Mycobacterium tuberculosis* complex
702 based on phylogenomics. *Open Res Eur.* 2021;1. doi:10.12688/openreseurope.14029.2

703 55. Chen Y, Takiff HE, Gao Q. Phenotypic instability of *Mycobacterium tuberculosis* strains
704 harbouring clinically prevalent drug-resistant mutations. *Lancet Microbe.* 2023;0.
705 doi:10.1016/S2666-5247(23)00007-1

706 56. Sirgel FA, Warren RM, Streicher EM, Victor TC, Helden PD van, Böttger EC. embB306
707 Mutations as Molecular Indicators to Predict Ethambutol Susceptibility in
708 *Mycobacterium tuberculosis*. *Chemotherapy.* 2013;58: 358–363.
709 doi:10.1159/000343474

710 57. Huo F, Ma Y, Li S, Xue Y, Shang Y, Dong L, et al. Specific *gyrA* Gene Mutations
711 Correlate with High Prevalence of Discordant Levofloxacin Resistance in
712 *Mycobacterium tuberculosis* Isolates from Beijing, China. *J Mol Diagn.* 2020;22: 1199–
713 1204. doi:10.1016/j.jmoldx.2020.06.010

714 58. Brankin AE, Fowler PW. Inclusion of minor alleles improves catalogue-based prediction
715 of fluoroquinolone resistance in *Mycobacterium tuberculosis*. *JAC-Antimicrob Resist.*
716 2023;5: dlad039. doi:10.1093/jacamr/dlad039

717 59. Nimmo C, Brien K, Millard J, Grant AD, Padayatchi N, Pym AS, et al. Dynamics of
718 within-host *Mycobacterium tuberculosis* diversity and heteroresistance during treatment.
719 *EBioMedicine.* 2020;55: 102747. doi:10.1016/j.ebiom.2020.102747

720 60. Perdigão J, Gomes P, Miranda A, Maltez F, Machado D, Silva C, et al. Using genomics to
721 understand the origin and dispersion of multidrug and extensively drug resistant
722 tuberculosis in Portugal. *Sci Rep.* 2020;10: 2600. doi:10.1038/s41598-020-59558-3

723 61. Singh A, Singh A, Grover S, Pandey B, Kumari A, Grover A. Wild-type catalase
724 peroxidase vs G279D mutant type: Molecular basis of Isoniazid drug resistance in

725 Mycobacterium tuberculosis. *Gene*. 2018;641: 226–234.
726 doi:10.1016/j.gene.2017.10.047

727 62. Vaziri F, Kohl TA, Ghajavand H, Kargarpour Kamakoli M, Merker M, Hadifar S, et al.
728 Genetic Diversity of Multi- and Extensively Drug-Resistant Mycobacterium
729 tuberculosis Isolates in the Capital of Iran, Revealed by Whole-Genome Sequencing. *J*
730 *Clin Microbiol*. 2019;57: e01477-18. doi:10.1128/JCM.01477-18

731 63. de Lourdes do Carmo Guimarães Diniz J, von Groll A, Unis G, Dalla-Costa ER, Rosa
732 Rossetti ML, Vianna JS, et al. Whole-genome sequencing as a tool for studying the
733 microevolution of drug-resistant serial Mycobacterium tuberculosis isolates.
734 *Tuberculosis*. 2021;131: 102137. doi:10.1016/j.tube.2021.102137

735 64. Altamirano M, Marostenmaki J, Wong A, FitzGerald M, Black WA, Smith JA. Mutations
736 in the catalase-peroxidase gene from isoniazid-resistant Mycobacterium tuberculosis
737 isolates. *J Infect Dis*. 1994;169: 1162–1165. doi:10.1093/infdis/169.5.1162

738 65. Ferrazoli L, Palaci M, da Silva Telles MA, Ueki SY, Kritski A, Marques LRM, et al.
739 Catalase Expression, katG, And MIC Of Isoniazid For Mycobacterium tuberculosis
740 Isolates From São Paulo, Brazil. *J Infect Dis*. 1995;171: 237–240.
741 doi:10.1093/infdis/171.1.237

742 66. Ramaswamy SV, Reich R, Dou S-J, Jasperse L, Pan X, Wanger A, et al. Single
743 Nucleotide Polymorphisms in Genes Associated with Isoniazid Resistance in
744 Mycobacterium tuberculosis. *Antimicrob Agents Chemother*. 2003;47: 1241–1250.
745 doi:10.1128/AAC.47.4.1241-1250.2003

746 67. Zhang Y, Heym B, Allen B, Young D, Cole S. The catalase—peroxidase gene and
747 isoniazid resistance of Mycobacterium tuberculosis. *Nature*. 1992;358: 591–593.
748 doi:10.1038/358591a0

749 68. Martinez E, Holmes N, Jelfs P, Sintchenko V. Genome sequencing reveals novel deletions
750 associated with secondary resistance to pyrazinamide in MDR Mycobacterium
751 tuberculosis. *J Antimicrob Chemother*. 2015;70: 2511–2514. doi:10.1093/jac/dkv128

752 69. Samarakoon H, Punchihewa S, Senanayake A, Hammond JM, Stevanovski I, Ferguson
753 JM, et al. Genopo: a nanopore sequencing analysis toolkit for portable Android devices.
754 *Commun Biol*. 2020;3: 1–5. doi:10.1038/s42003-020-01270-z

755 70. Gómez-González PJ, Perdigao J, Gomes P, Puyen ZM, Santos-Lazaro D, Napier G, et al.
756 Genetic diversity of candidate loci linked to Mycobacterium tuberculosis resistance to
757 bedaquiline, delamanid and pretomanid. *Sci Rep*. 2021;11: 19431. doi:10.1038/s41598-
758 021-98862-4

759 71. Schena E, Nedialkova L, Borroni E, Battaglia S, Cabibbe AM, Niemann S, et al.
760 Delamanid susceptibility testing of Mycobacterium tuberculosis using the resazurin
761 microtitre assay and the BACTEC™ MGIT™ 960 system. *J Antimicrob Chemother*.
762 2016;71: 1532–1539. doi:10.1093/jac/dkw044

763 72. Gomes LC, Campino S, Marinho CRF, Clark TG, Phelan JE. Whole genome sequencing
764 reveals large deletions and other loss of function mutations in Mycobacterium

765 tuberculosis drug resistance genes. *Microb Genomics*. 2021;7: 000724.
766 doi:10.1099/mgen.0.000724

767 73. De Maio F, Cingolani A, Bianco DM, Salustri A, Palucci I, Sanguinetti M, et al. First
768 description of the katG gene deletion in a *Mycobacterium tuberculosis* clinical isolate
769 and its impact on the mycobacterial fitness. *Int J Med Microbiol*. 2021;311: 151506.
770 doi:10.1016/j.ijmm.2021.151506

771 74. Ang MLT, Zainul Rahim SZ, de Sessions PF, Lin W, Koh V, Pethe K, et al. EthA/R-
772 Independent Killing of *Mycobacterium tuberculosis* by Ethionamide. *Front Microbiol*.
773 2017;8. doi:10.3389/fmicb.2017.00710

774 75. The CRyPTIC Consortium and the 100,000 Genomes Project. Prediction of Susceptibility
775 to First-Line Tuberculosis Drugs by DNA Sequencing. *N Engl J Med*. 2018;379: 1403–
776 1415. doi:10.1056/NEJMoa1800474

777 76. Köser CU, Cirillo DM, Miotto P. How To Optimally Combine Genotypic and Phenotypic
778 Drug Susceptibility Testing Methods for Pyrazinamide. *Antimicrob Agents Chemother*.
779 2020;64: e01003-20. doi:10.1128/AAC.01003-20

780 77. Yadon AN, Maharaj K, Adamson JH, Lai Y-P, Sacchettini JC, Ioerger TR, et al. A
781 comprehensive characterization of PncA polymorphisms that confer resistance to
782 pyrazinamide. *Nat Commun*. 2017;8: 588. doi:10.1038/s41467-017-00721-2

783 78. Park S-C, Lee K, Kim YO, Won S, Chun J. Large-Scale Genomics Reveals the Genetic
784 Characteristics of Seven Species and Importance of Phylogenetic Distance for
785 Estimating Pan-Genome Size. *Front Microbiol*. 2019;10. doi:10.3389/fmicb.2019.00834

786